1 **Cloning of the rice *Xo1* resistance gene and interaction of the Xo1 protein with**

2 **the defense-suppressing *Xanthomonas* effector Tal2h**

3

4 Andrew C. Read,[1†] Mathilde Hutin,[1,2†] Matthew J. Moscou,[3] Fabio C. Rinaldi,[1] and

5 Adam J. Bogdanove[1]*

6

7 [1] Plant Pathology and Plant-Microbe Biology Section, School of Integrative Plant

8 Science, Cornell University, Ithaca, NY 14853

9 [2] IRD, CIRAD, Université Montpellier, IPME, 34000 Montpellier, France

10 [3] The Sainsbury Laboratory, University of East Anglia, Norwich Research Park, Norwich,

11 NR4 7UK, United Kingdom

12 [†] These authors contributed equally.

13 Current address for F. C. Rinaldi: Vertex Pharmaceuticals, 50 Northern Avenue, Boston,

14 MA 02210

15 * Corresponding author: A. J. Bogdanove; ajb7@cornell.edu

16

20

26

27   **Abstract**

28

29   The *Xo1* locus in the heirloom rice variety Carolina Gold Select confers resistance to

30   bacterial leaf streak and bacterial blight, caused by *Xanthomonas oryzae* pvs. oryzicola

31   and oryzae, respectively. Resistance is triggered by pathogen-delivered transcription

32   activator-like effectors (TALEs) independent of their ability to activate transcription and

33   is suppressed by variants called truncTALEs common among Asian strains. By

34   transformation of the susceptible variety Nipponbare, we show that one of 14

35   nucleotide-binding, leucine-rich repeat (NLR) protein genes at the locus, with a zfBED

36   domain, is the *Xo1* gene. Analyses of published transcriptomes revealed that the *Xo1*-

37   mediated response is more similar to those mediated by two other NLR resistance

38   genes than it is to the response associated with TALE-specific transcriptional activation

39   of the executor resistance gene *Xa23*, and that a truncTALE dampens or abolishes

40   activation of defense-associated genes by *Xo1*. In *Nicotiana benthamiana* leaves,

41   fluorescently-tagged Xo1 protein, like TALEs and truncTALEs, localized to the nucleus.

42   And, endogenous Xo1 specifically co-immunoprecipitated from rice leaves with a

43   pathogen-delivered, epitope-tagged truncTALE. These observations suggest that

44   suppression of Xo1-function by truncTALEs occurs through direct or indirect physical

45   interaction. They further suggest that effector co-immunoprecipitation may be effective

46   for identifying or characterizing other resistance genes.

47

48

49   Bacterial leaf streak of rice, caused by *Xanthomonas oryzae* pv. oryzicola (Xoc), is an

50   increasing threat to production in many parts of the world, especially in Africa. Bacterial

51   blight of rice, caused by *X. oryzae* pv. oryzae (Xoo) has long been a major constraint in

52   Asia and is becoming prevalent in Africa. The purified American heirloom rice variety

53   Carolina Gold Select (hereafter Carolina Gold; McClung and Fjellstrom, 2010) is

54   resistant to all tested African strains of Xoc and some tested strains of Xoo (Read et al.,

55   2016). Using an African strain of Xoc, the resistance was mapped to chromosome 4 and

56   designated as *Xo1* (Triplett et al., 2016). Both Xoc and Xoo deploy multiple type III-

57   secreted transcription activator-like effectors (TALEs) during infection. TALEs enter the

58   plant nucleus and bind to promoters, each with different sequence specificity, to

59   transcriptionally activate effector-specific target genes (Perez-Quintero and Szurek,

60   2019). Some of these genes, called susceptibility genes, contribute to disease

61   development (Hutin et al., 2015). In some host genotypes, a TALE may activate a so-

62   called executor resistance gene, leading to host cell death that stops the infection

63   (Bogdanove et al., 2010). Most of the cloned resistance genes for bacterial blight are in

64   fact executor genes (Zhang et al., 2015). *Xo1* is different. It mediates resistance in

65   response to TALEs with distinct DNA-binding specificities independent of their ability to

66   activate transcription (Triplett et al., 2016). Also, unlike executor genes, *Xo1* function is

67   suppressed by a variant class of these effectors known as truncTALEs (also called

68   iTALEs). Like TALEs, TruncTALEs nuclear localize (Ji et al., 2016), however due to

69   large N and C terminal deletions they do not bind DNA (Read et al., 2016).

70   *Xo1* maps to a region that in the reference rice genome (cv. Nipponbare)

71   contains seven nucleotide-binding, leucine-rich repeat protein genes ("NLR" genes)

72   (Triplett et al., 2016). NLR genes are the largest class of plant disease resistance

73   genes. NLR proteins recognize specific, corresponding pathogen effector proteins

74   through direct interaction or by detecting effector-dependent changes of host target

75   proteins, and mediate downstream defense signaling that leads to expression of

76   defense genes and a programmed localized cell death, the hypersensitive reaction (HR)

77   (Lolle et al., 2020). Recently, by whole genome sequencing, we determined that the

78   *Xo1* locus in Carolina Gold comprises 14 NLR genes. We identified one of these, *Xo1$_{11}$*,

79   as a strong candidate based on its structural similarity to the previously cloned and only

80   known NLR resistance gene for bacterial blight, *Xa1* (Read et al., 2020). *Xa1*, originally

81   identified in the rice variety Kogyoku, maps to the same location (Yoshimura et al.,

82   1998) and behaves similarly to *Xo1*: it mediates recognition of TALEs with distinct DNA-

83   binding specificities (and thus confers resistance also to bacterial leaf streak), and its

84   activity is suppressed by truncTALEs (Ji et al., 2016). *Xo1$_{11}$* and *Xa1* are members of a

85   small subfamily of NLR genes that encode an unusual N-terminal domain comprising a

86   zinc finger BED (zfBED) motif (Read et al., 2020).

87   To ascertain whether *Xo1$_{11}$* is the gene responsible for *Xo1* resistance, we

88   generated transgenic Nipponbare plants expressing it. For transformation, we amplified

89   the genomic *Xo1$_{11}$* coding sequence (5,882 bp) as well as the 993 bp region upstream

90   of the start codon and cloned them together into a binary vector with a 35S terminator.

91   T0 $Xo1_{11}$ plants were inoculated by syringe infiltration with African Xoc strain

92   CFBP7331, which has no truncTALE of its own, carrying either an empty vector (EV) or

93   the plasmid-borne truncTALE gene *tal2h* (p2h) from the Asian Xoc strain BLS256 (Read

94   et al., 2016). Phenotypes of CFBP7331(EV) and CFBP7331(p2h) were confirmed on

95   untransformed Nipponbare and Carolina Gold plants (**Fig. S1**). Plants from two $Xo1_{11}$

96   transformation events displayed resistance to the strain with the EV, but not to the strain

97   carrying Tal2h (**Fig. 1**), demonstrating that $Xo1_{11}$ is the *Xo1* gene.

98   NLR protein activation is characteristically followed by a suite of responses that

99   includes massive transcriptional reprogramming leading both to HR and to activation of

100   a large number of defense-associated genes (Cui et al., 2015). To gain insight into the

101   nature of *Xo1*-mediated resistance, we compared the global profile of differentially

102   expressed genes during *Xo1*-mediated defense to those of two other NLR genes in rice

103   and to the profile associated with an executor gene. We used our previously reported

104   RNAseq data from Carolina Gold plants inoculated with CFBP7331(EV) or mock

105   inoculum (Read et al., 2020), data for the NLR gene *Pia* for resistance to the rice blast

106   pathogen *Magnaporthe oryzae* (Tanabe et al., 2014), data from rice resistant to

107   bacterial leaf streak due to transgenic expression of the maize NLR gene *Rxo1* (Xie et

108   al., 2007; Zhou et al., 2010), and data for the transcriptomic response associated with

109   induction of the executor resistance gene *Xa23* by an Xoo strain with the corresponding

110   TALE (Tariq et al., 2018). Though limited, these datasets include the only currently

111   available expression data for NLR and executor gene-mediated resistance to

112   *Xanthomonas* in rice. Differentially expressed genes ($\log_2$-fold change >1 or <-1; *p*-

113   value >0.05) in the comparison between pathogen-inoculated and mock-inoculated

114   plants were compared across the four datasets. The total number of DEGs ranged from

115   10,050 for *Xo1* to 628 for *Xa23*, and the overall profiles were largely distinct (**Fig. 2A**,

116   **Table S1**). For each resistance gene, there were a number of DEGs found only in the

117   pathogen to mock comparison for that dataset, and this was highest for *Xo1* (7,121

118   genes) (**Fig. 2A, Table S1**). Differences among the overall DEG profiles may be

119   influenced by the expression assay (RNAseq vs. microarray), pathogen, annotation, or

120   timepoints used. To compare the responses further the expression of 340 rice genes

121   associated with plant defense response (gene ontology group 0006952) was examined.

122   The *Xo1* profile comprised the largest number of plant defense DEGs (99) and had

123   more DEGs in common with the other NLR-mediated responses (16 with *Rxo1* and 26

124   with *Pia*) than with the executor gene response (8) (Fig. 2B). Additionally, each of the

125   NLR-mediated responses resulted in a larger number of differentially expressed

126   defense genes (26 for *Rxo1*, 41 for *Pia*) than the *Xa23* response (14), and based on

127   principle component analysis of the defense DEG profiles, were more similar to one

128   another than to the executor gene response (**Fig. 2B and C** and **Table S2**).

129   We also compared DEGs relative to mock in Carolina Gold plants inoculated with

130   CFBP7331(EV) and Carolina Gold plants inoculated with CFBP7331(p2h) (Read et al.,

131   2020), to gain insight into how *Xo1*-mediated resistance is overcome by a pathogen

132   delivering a truncTALE. In contrast to the 99 defense response genes differentially

133   expressed in response to CFBP7331(EV), only 18 defense genes were differentially

134   expressed in response to CFBP7331(p2h) (**Fig. 2D**). Of these 18 genes, 7 were

135   differentially expressed only in the response to the strain with *tal2h*, 4 up and 3 down.

136   Of the remaining 11, 4 were up and 2 were down in both responses, but each less so in

137   the response to the strain with *tal2h*. The other 5 moved in opposite directions entirely,

138   up in the absence but repressed in the presence of *tal2h*, relative to mock. This

139   expression profile during suppression of *Xo1*-mediated resistance is consistent with

140   Tal2h functioning early in the defense cascade. The bacterial leaf streak susceptibility

141   gene *OsSULTR3;6* (Cernadas et al., 2014), activated by Tal8e of CFBP7331 (Wilkins et

142   al., 2015), is strongly induced by both CFBP7331(EV) and CFBP7331(p2h) (**Table S3**),

143   indicating that TALE function is not compromised by Xo1 or by Tal2h.

144   The observation that Xo1 reprograms transcription of canonical defense genes

145   upon recognition of the cognate pathogen effector and that reprogramming by Xo1 is

146   essentially blocked by Tal2h led us to explore whether Xo1 localizes to the same

147   subcellular location as TALEs and truncTALEs. Some, but not all, NLR proteins nuclear

148   localize (Shen et al., 2007; Wirthmueller et al., 2007; Caplan et al., 2008; Cheng et al.,

149   2009), and we previously identified putative nuclear localization signals (NLSs) in $Xo1_{11}$

150   (Read et al., 2020). We generated expression constructs for a green fluorescent protein

151   (GFP) fusion to the N-terminus of Xo1 as well as an N-terminal monomeric red

152   fluorescent protein (mRFP) fusion both to a TALE (Tal1c of Xoc BLS256) and to Tal2h.

153   These constructs were delivered into *Nicotiana benthamiana* leaves using *A.*

154   *tumefaciens* strain GV3101, and the leaves imaged with a Zeiss 710 confocal

155   microscope (**Fig. 3**). GFP-Xo1 in the absence of either effector but with free mRFP

156   localized to foci that appeared to be nuclei. Co-expression with mRFP-Tal1c or with

157   mRFP-Tal2h confirmed that these foci were nuclei.

158   The localization of Xo1, the TALE, and the truncTALE to the nucleus when

159   transiently expressed in *N. benthamiana* led us to pursue the hypothesis that Xo1

160   physically interacts with one or both of these proteins in the native context. We

161   generated plasmid constructs that add a 3x FLAG tag to the C-terminus of TALE Tal1c

162   or the truncTALE Tal2h (Tal1c-FLAG and Tal2h-FLAG) and introduced them individually

163   into the TALE-deficient *X. oryzae* strain X11-5A (Triplett et al., 2011) for co-

164   immunoprecipitation from inoculated Carolina Gold leaves (**Fig. 4**). Abilities of the

165   tagged TALE and truncTALE to respectively trigger and suppress *Xo1*-mediated

166   resistance were confirmed (**Fig. S2**). We included also a plasmid for expression of a

167   second, untagged TALE (Tal3c from BLS256) and a plasmid for untagged Tal2h. By

168   pairing the X11-5A transformants with each other or with the untransformed control

169   strain, we were able to probe for Carolina Gold proteins interacting with the tagged

170   TALE or truncTALE, and for interactions of these proteins with each other or with the

171   second TALE. Select combinations were inoculated to Nipponbare leaves for

172   comparison. Inoculation was done by syringe infiltration, in 30-40 contiguous spots on

173   each side of the leaf midrib. For each co-inoculation, tissue was harvested at 48 hours

174   and ground in liquid N_2, then soluble extract was incubated with anti-FLAG agarose

175   beads and washed to immunopurify the tagged and interacting proteins.

176   Immunoprecipitates were eluted, and an aliquot of each was subjected to western

177   blotting with anti-TALE antibody (**Fig. S3**). The remainders were then resolved on a 4-

178   20% SDS-PAGE and eluates from gel slices containing proteins between approximately

179   60 and 300 kDa (**Fig. S4**) were digested and the peptides analyzed by mass

180   spectrometry. Proteins were considered present in a sample if at least three peptides

181   mapped uniquely to any of the pertinent annotated genomes searched: the *X. oryzae*

182   strain X11-5A genome (Triplett et al., 2011) plus the TALE(s) or TruncTALE being

183   expressed, the Nipponbare genome (MSU 7; Kawahara et al., 2013), and the Carolina

184   Gold genome (Read et al., 2020). For the Carolina Gold genome, we re-annotated

185   using the RNAseq data from CFBP7331(EV), CFBP7331(p2h), and mock-inoculated

186   plants cited earlier. We carried out the experiment twice.

187   In the western blot for each experiment (**Fig. S3**), we detected the tagged TALE

188   or truncTALE in each corresponding sample, with the exception of a Tal1c-

189   FLAG/Tal3c/Nipponbare sample in the first experiment. No Tal3c or untagged Tal2h

190   was detected in any sample. The mass spectrometry confirmed these observations,

191   suggesting that neither TALEs with truncTALEs nor TALEs with other TALEs interact

192   appreciably (**Fig. 4**). Xo1 was consistently detected in the Carolina Gold/Tal2h-FLAG

193   samples, irrespective of any co-delivered Tal1c or Tal3c, and not in the Tal1c-FLAG

194   samples or any other sample (**Fig. 4**). No other protein consistently co-purified with

195   Tal2h-FLAG or Tal1c-FLAG in either Carolina Gold or Nipponbare samples (**Dataset**

196   **S1**).

197   In summary, we have shown that 1) an NLR protein gene at the *Xo1* locus,

198   harboring an integrated zfBED domain, is *Xo1*; 2) the *Xo1*-mediated response is more

199   similar to those mediated by two other NLR resistance genes than it is to the response

200   associated with TALE-specific transcriptional activation of an executor resistance gene;

201   3) a truncTALE abolishes or dampens activation of defense-associated genes by *Xo1*;

202   4) the Xo1 protein, like TALEs and truncTALEs, localizes to the nucleus, and 5) Xo1

203   specifically co-immunoprecipitates from rice leaves with a pathogen-delivered, epitope-

204   tagged truncTALE. Thus, *Xo1* is an allele or paralog of *Xa1*, and suppression of Xo1

205   function by a truncTALE is likely the result of physical interaction between the

206 resistance protein and the effector. The latter prediction is consistent with the Xo1 DEG

207 profile during suppression by Tal2h, which suggested that Tal2h functions early in the

208 defense cascade, perhaps by blocking TALE recognition by Xo1.

209 Whether the interaction between Tal2h and Xo1 is direct or indirect is not certain,

210 but the fact that no other protein was detected consistently that co-immunoprecipitated

211 with Tal2h and Xo1 suggests the interaction is direct. It is tempting to speculate also

212 that TALEs trigger Xo1-mediated resistance by direct interaction with the protein and

213 that truncTALEs function by disrupting the association. Though Tal1c did not pull down

214 Xo1, this might be explained by its lower apparent abundance, based on the western

215 blots. Tal1c might interact weakly or transiently with Xo1, or any complex of the proteins

216 in the plant cells may have begun to degrade with the developing HR at the 48 hour

217 time point sampled. It is also possible that Tal2h interacts with TALEs and masks them

218 from the resistance protein, but both our co-immunoprecipitation results and the fact

219 that Tal2h does not impact TALE activation of the *OsSULTR3;6* susceptibility suggest

220 that this is not the case. An alternative hypothesis is that Xo1 recognition of TALEs is

221 not mediated by a direct interaction between the two proteins.

222 The results presented constitute an important step toward understanding how

223 Xo1 works, and how its function can be suppressed by the pathogen. Toward

224 determining the relationship of the interaction to defense suppression, an immediate

225 next step might be structure function analysis of the interaction to determine the

226 portion(s) of Xo1 and Tal2h involved. For Xo1, the LRR may be the determinative

227 interacting domain. Our previous comparison of the motifs present in $Xo1_{11}$, Xa1, and

228 the closest Nipponbare homolog (Nb-$xo1_5$, which is expressed) revealed that the zfBED

229   and CC domains are identical and the NB-ARC domains nearly so (Read et al., 2020).

230   In contrast, the leucine rich repeat domain of Nb-xo1$_5$ differs markedly from those of

231   Xo1 and Xa1, which, with the exception of an additional repeat in Xa1, are very similar.

232   Supporting this hypothesis, differences in the LRR determine the pathogen race

233   specificities of some flax rust resistance genes (Ellis et al., 1999). More broadly, the

234   ability of tagged Tal2h to pull down Xo1 suggests that effector co-immunoprecipitation

235   may be an effective approach to characterizing pathogen recognition mechanisms of

236   other resistance proteins, or for identifying a resistance gene *de novo*.

237   While this paper was under review, Ji and colleagues (Ji et al., 2020) reported

238   the cloning and functional characterization of several *Xa1* homologs, which also

239   demonstrated that *Xo1$_{11}$* is *Xo1*.

240

241

242   **Figure legends**

243

244   **Fig. 1.** Transgenic Nipponbare plants expressing Xo1$_{11}$ are resistant to African Xoc

245   strain CFBP7331 and the resistance suppressed by a truncTALE. Susceptible cultivar

246   Nipponbare was transformed with pAR902, and leaves of T0 plants from two events

247   were syringe-infiltrated with African Xoc strain CFBP7311 carrying either empty vector

248   (EV) or *tal2h* (p2h) adjusted to OD$_{600}$ 0.4. Leaves were photographed on a light box at 4

249   days after inoculation. Resistance is apparent as HR (necrosis) at the site of inoculation

250   and disease as expanded, translucent watersoaking.

251

252   **Fig. 2.** The Xo1-mediated transcriptomic response is similar to those of other NLR

253   genes and is essentially eliminated by Tal2h. **A,** Expression heatmaps (columns)

254   showing all differentially expressed genes (DEGs) in plants undergoing the resistant

255   response compared to mock inoculated plants for *Xo1*, the NLR genes *Pia* and *Rxo1*,

256   and the executor resistance gene *Xa23*. White numbers for each on the heatmap

257   indicate the number of DEGs specific to each response (see **Table S1**). Total numbers

258   of DEGs are indicated below. **B,** Heatmaps for the subset of DEGs from (A) that belong

259   to gene ontology group 0006952, defense response, with totals displayed at bottom. C,

260   Principal component analysis. The first two principal components (PC) explain 54.0%

261   and 31.6% of the variation with a total of 85.6%. PC1 demarcated two major clusters: 1)

262   *Xo1*, *Pia*, and *Rxo1*, and 2) *Xa23* **D,** Heatmaps for the 18 defense response DEGs

263   identified in the comparison of Carolina Gold plants inoculated with CFBP7331(p2h) to

264   mock inoculated plants. The "EV" heatmap shows their expression relative to mock in

265   Carolina Gold plants inoculated with CFBP7331(EV) (resistance), and the "p2h" column

266   shows their expression relative to mock in the presence of Tal2h (disease). The DEGs

267   have been divided into five categories: **I**, induced in both; **II**, down-regulated in both; **III**,

268   induced in resistance and down-regulated in disease; **IV**, not differentially expressed in

269   resistance and induced in disease; and **V**, not differentially expressed in resistance and

270   down-regulated in disease.

271

272   **Fig. 3.** Xo1 localizes to the nucleus. Using *Agrobacterium* co-infiltrations, an expression

273   construct for Xo1 with GFP at the N-terminus (GFP-Xo1) together with a p19 silencing

274   suppressor construct were introduced into *Nicotiana benthamiana* leaves alone or with

275 a construct for mRFP, mRFP fused to TALE Tal1c (mRFP-Tal1c), or mRFP fused to the

276 truncTALE Tal2h (mRFP-Tal2h). Confocal image stacks were taken at 3 days after

277 inoculation and are presented as maximum intensity projections. Insets are

278 magnifications of individual nuclei. The scale bars represent 50 μm.

279

280 **Fig. 4.** Xo1 co-immunoprecipitates with Tal2h. **Top,** strategy used for co-

281 immunoprecipitation (Co-IP) of truncTALE Tal2h or TALE Tal1c and any interactors.

282 Plasmid borne expression constructs for Tal2h or Tal1c with a C-terminal 3x FLAG tag,

283 as well as untagged Tal2h and a second TALE,Tal3c were introduced into

284 *Xanthomonas oryzae* strain X11-5. Paired combinations of the transformants with each

285 other or with the untransformed control strain, or the control strain alone, were co-

286 infiltrated into leaves of rice varieties Carolina Gold and Nipponbare at a final OD_{600} 0.5

287 for each transformant. Samples were collected 48 hours after inoculation, ground, and

288 sonicated before Co-IP using anti-FLAG agarose beads. After elution and SDS-PAGE

289 separation, proteins between approximately 60 and 300 kDa were eluted, digested and

290 analyzed by mass spectrometry. The experiment was conducted twice. **Bottom**, co-IP

291 results. For each immunoprecipitate, the numbers of unique peptides detected that

292 matched Tal2h, Tal3c, Tal1c, or Xo1 in each experiment are shown. "-" indicates that ≤

293 2 unique peptides were detected.

294

295

296 **Acknowledgments**

297

312

313

314   **Author contributions**

315

316   AR, MH, FR, and AB conceived and designed the study; AR, MH, and FR carried out

317   the experiments; AR, MH, FR, MM, and AB analyzed data; AR, MH, and AB wrote the

318   manuscript.

319

320

321   **Supplemental files**

322

323   **1. Supplemental text and figures**

324

325   **Materials and methods**

326

327   **Fig. S1.** Confirmation of CFBP7331(EV) and CFBP(p2h) inoculum on

328   Nipponbare and Carolina Gold plants.

329

330   **Fig. S2.** Symptoms on Carolina Gold and Nipponbare leaves caused by

331   inoculum used for the co-IP experiments.

332

333   **Fig. S3.** Western blot of immunoprecipitates using anti-TALE antibody.

334

335   **Fig. S4.** SDS-PAGE of immunoprecipitates and size range excised for mass

336   spectrometry.

337

338   **Supplemental references**

339

340   **2. Supplemental tables**

341

342   **Table S1.** DEGs in Fig. 2A (all DEGS)

343

344   **Table S2.** DEGs in Fig. 2B (GO:0006952 DEGs)

345

346   **Table S3.** DEGs in Fig. 2C (GO:0006952 in disease) and *S* gene *OsSULTR3;6*

347   (LOC_ Os01g52130) expression

348

349   **3. Dataset S1.** Mass spectrometry data

350

351

352   **References**

353

354   Bogdanove, A.J., Schornack, S., and Lahaye, T. 2010. TAL effectors: finding plant

355   genes for disease and defense. Curr. Opin. Plant Biol. 13:394-401.

356   Caplan, J.L., Mamillapalli, P., Burch-Smith, T.M., Czymmek, K., and Dinesh-Kumar,

357   S.P. 2008. Chloroplastic protein NRIP1 mediates innate immune receptor

358   recognition of a viral effector. Cell 132:449-462.

359   Cernadas, R.A., Doyle, E.L., Nino-Liu, D.O., Wilkins, K.E., Bancroft, T., Wang, L.,

360   Schmidt, C.L., Caldo, R., Yang, B., White, F.F., Nettleton, D., Wise, R.P., and

361   Bogdanove, A.J. 2014. Code-assisted discovery of TAL effector targets in

362   bacterial leaf streak of rice reveals contrast with bacterial blight and a novel

363   susceptibility gene. PLoS Path. 10:e1003972.

364   Cheng, Y.T., Germain, H., Wiermer, M., Bi, D., Xu, F., Garcia, A.V., Wirthmueller, L.,

365   Despres, C., Parker, J.E., Zhang, Y., and Li, X. 2009. Nuclear pore complex

366   component MOS7/Nup88 is required for innate immunity and nuclear

367   accumulation of defense regulators in Arabidopsis. Plant Cell 21:2503-2516.

368   Cui, H., Tsuda, K., and Parker, J.E. 2015. Effector-triggered immunity: from pathogen

369   perception to robust defense. Annu. Rev. Plant Biol. 66:487-511.

370   Ellis, J.G., Lawrence, G.J., Luck, J.E., and Dodds, P.N. 1999. Identification of regions in

371   alleles of the flax rust resistance gene *L* that determine differences in gene-for-

372   gene specificity. Plant Cell 11:495-506.

373   Hutin, M., Perez-Quintero, A.L., Lopez, C., and Szurek, B. 2015. MorTAL Kombat: the

374   story of defense against TAL effectors through loss-of-susceptibility. Front. Plant

375   Sci. 6:535.

376   Ji, C., Ji, Z., Liu, B., Cheng, H., Liu, H., Liu, S., Yang, B., and Chen, G. 2020. *Xa1* allelic

377   *R* genes activate rice blight resistance suppressed by Interfering TAL effectors.

378   Plant Communications:100087.

379   Ji, Z., Ji, C., Liu, B., Zou, L., Chen, G., and Yang, B. 2016. Interfering TAL effectors of

380   *Xanthomonas oryzae* neutralize *R*-gene-mediated plant disease resistance. Nat.

381   Commun. 7:13435.

382   Kawahara, Y., de la Bastide, M., Hamilton, J.P., Kanamori, H., McCombie, W.R.,

383   Ouyang, S., Schwartz, D.C., Tanaka, T., Wu, J., and Zhou, S. 2013.

384   Improvement of the *Oryza sativa* Nipponbare reference genome using next

385   generation sequence and optical map data. Rice 6:4.

386   Lolle, S., Stevens, D., and Coaker, G. 2020. Plant NLR-triggered immunity: from

387   receptor activation to downstream signaling. Curr. Opin. Immunol. 62:99-105.

388 McClung, A., and Fjellstrom, R. 2010. Using molecular genetics as a tool to identify and

389   refine "Carolina Gold". Pages 37-41 in: The Golden Seed: Writings on the History

390   and Culture of Carolina Gold Rice, D.S. Shields, ed. Douglas W. Bostick for the

391   Carolina Gold Rice Foundation.

392 Perez-Quintero, A.L., and Szurek, B. 2019. A decade decoded: spies and hackers in the

393   history of TAL effectors research. Annu. Rev. Phytopathol. 57:459-481.

394 Read, A.C., Rinaldi, F.C., Hutin, M., He, Y.Q., Triplett, L.R., and Bogdanove, A.J. 2016.

395   Suppression of *Xo1*-mediated disease resistance in rice by a truncated, non-

396   DNA-binding TAL effector of *Xanthomonas oryzae*. Front. Plant Sci. 7:1516.

397 Read, A.C., Moscou, M.J., Zimin, A.V., Pertea, G., Meyer, R.S., Purugganan, M.D.,

398   Leach, J.E., Triplett, L.R., Salzberg, S.L., and Bogdanove, A.J. 2020. Genome

399   assembly and characterization of a complex zfBED-NLR gene-containing

400   disease resistance locus in Carolina Gold Select rice with Nanopore sequencing.

401   PLoS Genet. 16:e1008571.

402 Shen, Q.H., Saijo, Y., Mauch, S., Biskup, C., Bieri, S., Keller, B., Seki, H., Ulker, B.,

403   Somssich, I.E., and Schulze-Lefert, P. 2007. Nuclear activity of MLA immune

404   receptors links isolate-specific and basal disease-resistance responses. Science

405   315:1098-1103.

406 Tanabe, S., Yokotani, N., Nagata, T., Fujisawa, Y., Jiang, C., Abe, K., Ichikawa, H.,

407   Mitsuda, N., Ohme-Takagi, M., Nishizawa, Y., and Minami, E. 2014. Spatial

408   regulation of defense-related genes revealed by expression analysis using

409   dissected tissues of rice leaves inoculated with *Magnaporthe oryzae*. J. Plant

410   Physiol. Pathol. 2:1000135.

411   Tariq, R., Wang, C., Qin, T., Xu, F., Tang, Y., Gao, Y., Ji, Z., and Zhao, K. 2018.

412   Comparative transcriptome profiling of rice near-isogenic line carrying *Xa23*

413   under infection of *Xanthomonas oryzae* pv. oryzae. Int. J. Mol. Sci. 19:717.

414   Triplett, L.R., Hamilton, J.P., Buell, C.R., Tisserat, N.A., Verdier, V., Zink, F., and Leach,

415   J.E. 2011. Genomic analysis of *Xanthomonas oryzae* isolates from rice grown in

416   the United States reveals substantial divergence from known *X. oryzae*

417   pathovars. Appl. Environ. Microbiol. 77:3930-3937.

418   Triplett, L.R., Cohen, S.P., Heffelfinger, C., Schmidt, C.L., Huerta, A.I., Tekete, C.,

419   Verdier, V., Bogdanove, A.J., and Leach, J.E. 2016. A resistance locus in the

420   American heirloom rice variety Carolina Gold Select is triggered by TAL effectors

421   with diverse predicted targets and is effective against African strains of

422   *Xanthomonas oryzae* pv. oryzicola. Plant J. 87:472-483.

423   Wilkins, K.E., Booher, N.J., Wang, L., and Bogdanove, A.J. 2015. TAL effectors and

424   activation of predicted host targets distinguish Asian from African strains of the

425   rice pathogen *Xanthomonas oryzae* pv. oryzicola while strict conservation

426   suggests universal importance of five TAL effectors. Front. Plant Sci. 6:536.

427   Wirthmueller, L., Zhang, Y., Jones, J.D., and Parker, J.E. 2007. Nuclear accumulation of

428   the Arabidopsis immune receptor RPS4 is necessary for triggering EDS1-

429   dependent defense. Curr. Biol. 17:2023-2029.

430   Xie, X.W., Yu, J., Xu, J.L., Zhou, Y.L., and Li, Z.K. 2007. [Introduction of a non-host

431   gene *Rxo1* cloned from maize resistant to rice bacterial leaf streak into rice

432   varieties]. Sheng Wu Gong Cheng Xue Bao 23:607-611.

433   Yoshimura, S., Yamanouchi, U., Katayose, Y., Toki, S., Wang, Z.X., Kono, I., Kurata,

434   N., Yano, M., Iwata, N., and Sasaki, T. 1998. Expression of *Xa1*, a bacterial

435   blight-resistance gene in rice, is induced by bacterial inoculation. Proc. Natl.

436   Acad. Sci. USA 95:1663-1668.

437   Zhang, J., Yin, Z., and White, F. 2015. TAL effectors and the executor *R* genes. Front.

438   Plant Sci. 6:641.

439   Zhou, Y.L., Xu, M.R., Zhao, M.F., Xie, X.W., Zhu, L.H., Fu, B.Y., and Li, Z.K. 2010.

440   Genome-wide gene responses in a transgenic rice line carrying the maize

441   resistance gene *Rxo1* to the rice bacterial streak pathogen, *Xanthomonas oryzae*

442   pv. oryzicola. BMC Genomics 11:78.

443

Xoc CFBP7331

Event 1
EV p2h

Event 2
EV p2h
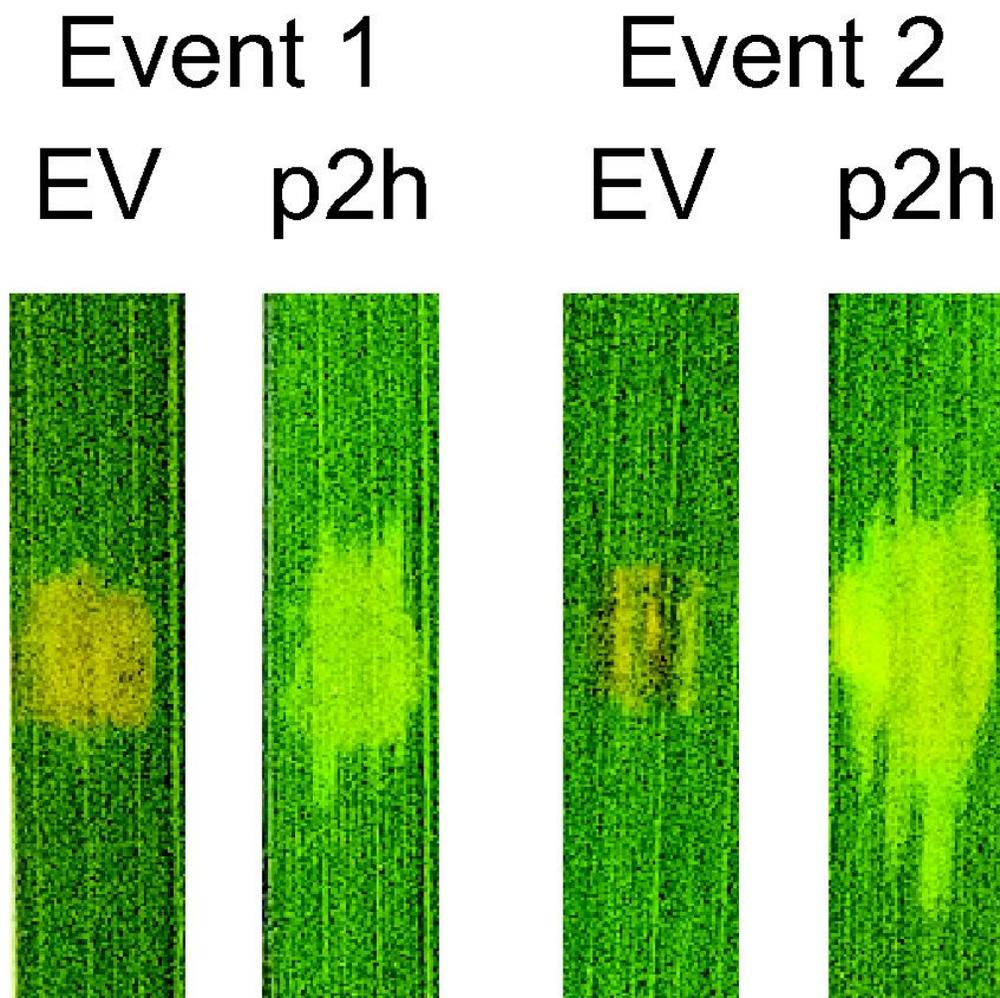
Fig. 1. Transgenic Nipponbare plants expressing $Xo1_{11}$ are resistant to African Xoc strain CFBP7331 and the resistance suppressed by a truncTALE. Susceptible cultivar Nipponbare was transformed with pAR902, and leaves of T0 plants from two events were syringe-infiltrated with African Xoc strain CFBP7311 carrying either empty vector (EV) or *tal2h* (p2h) adjusted to OD600 0.4. Leaves were photographed on a light box at 4 days after inoculation. Resistance is apparent as HR (necrosis) at the site of inoculation and disease as expanded, translucent watersoaking.

35x42mm (600 x 600 DPI)
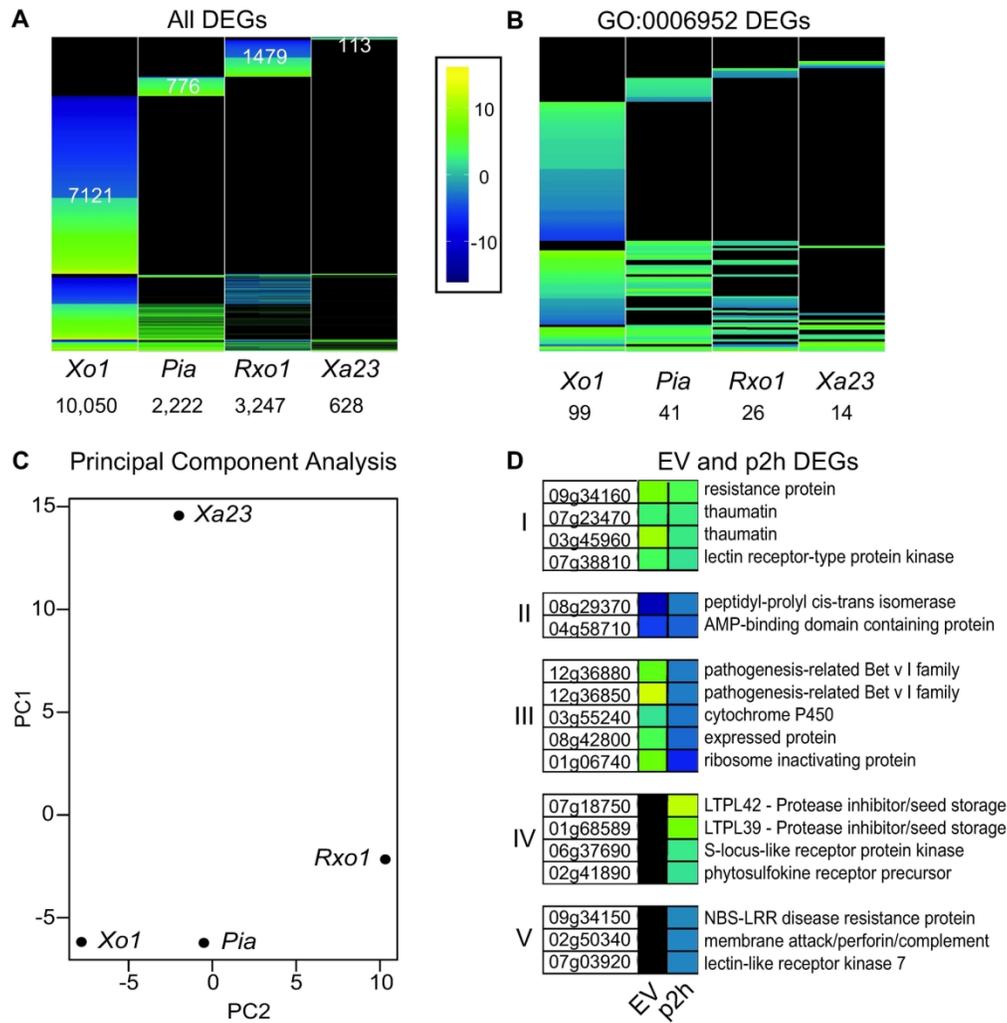
Fig. 2. The Xo1-mediated transcriptomic response is similar to those of other NLR genes and is essentially eliminated by Tal2h. A, Expression heatmaps (columns) showing all differentially expressed genes (DEGs) in plants undergoing the resistant response compared to mock inoculated plants for Xo1, the NLR genes Pia and Rxo1, and the executor resistance gene Xa23. White numbers for each on the heatmap indicate the number of DEGs specific to each response (see Table S1). Total numbers of DEGs are indicated below. B, Heatmaps for the subset of DEGs from (A) that belong to gene ontology group 0006952, defense response, with totals displayed at bottom. C, Principal component analysis. The first two principal components (PC) explain 54.0% and 31.6% of the variation with a total of 85.6%. PC1 demarcated two major clusters: 1) Xo1, Pia, and Rxo1, and 2) Xa23 D, Heatmaps for the 18 defense response DEGs identified in the comparison of Carolina Gold plants inoculated with CFBP7331(p2h) to mock inoculated plants. The "EV" heatmap shows their expression relative to mock in Carolina Gold plants inoculated with CFBP7331(EV) (resistance), and the "p2h" column shows their expression relative to mock in the presence of Tal2h (disease). The DEGs have been divided into five categories: I, induced in both; II, down-regulated in both; III, induced in resistance and down-regulated in disease; IV, not differentially expressed in resistance and induced in disease; and V, not differentially expressed in resistance and down-regulated in disease.

170x174mm (300 x 300 DPI)
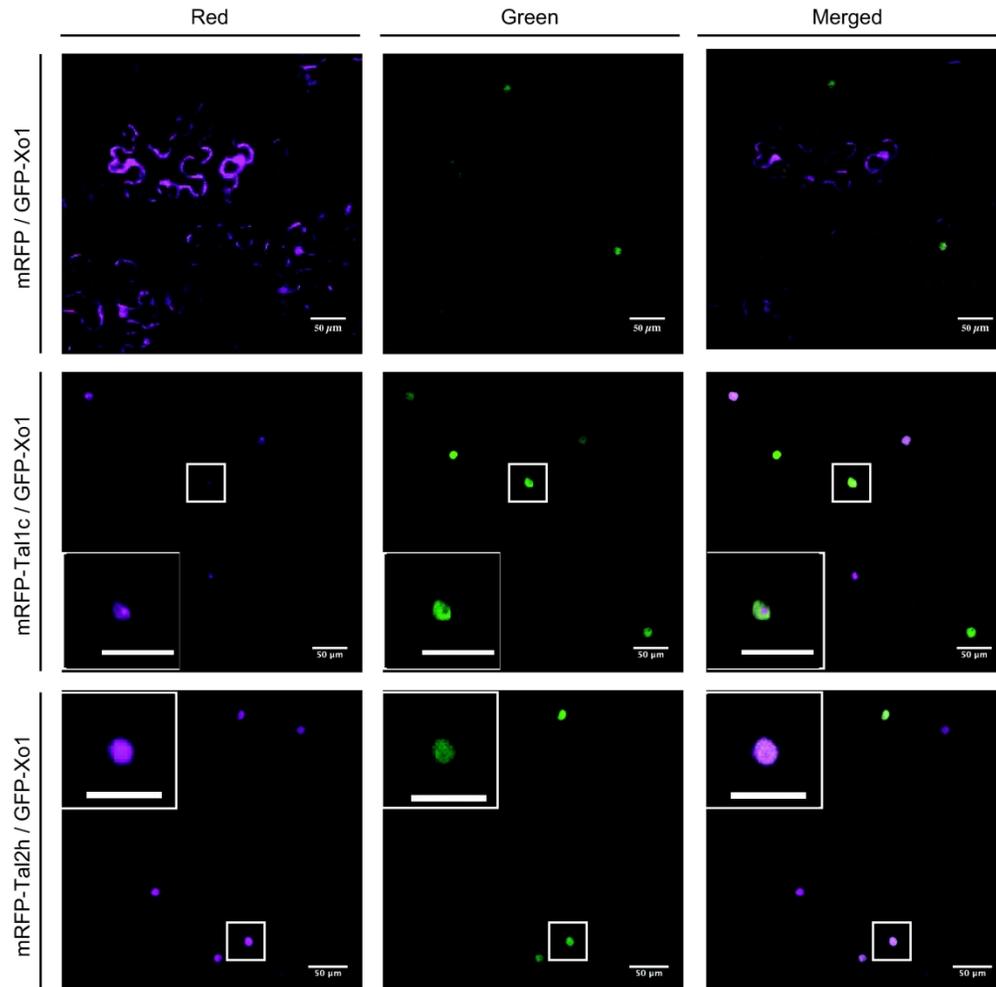
Fig. 3. Xo1 localizes to the nucleus. Using *Agrobacterium* co-infiltrations, an expression construct for Xo1 with GFP at the N-terminus (GFP-Xo1) together with a p19 silencing suppressor construct were introduced into *Nicotiana benthamiana* leaves alone or with a construct for mRFP, mRFP fused to TALE Tal1c (mRFP-Tal1c), or mRFP fused to the truncTALE Tal2h (mRFP-Tal2h). Confocal image stacks were taken at 3 days after inoculation and are presented as maximum intensity projections. Insets are magnifications of individual nuclei. The scale bars represent 50 µm.

168x166mm (600 x 600 DPI)

Input			Carolina Gold										Nipponbare					
			Tal2h		Tal2h / Tal3c		Tal1c		Tal1c / Tal2h				Tal2h / Tal3c		Tal1c / Tal3c	
Experiment	#1	#2	#1	#2	#1	#2	#1	#2	#1	#2	#1	#2	#1	#2	#1	#2
Tal2h	-	-	5	16	7	13	-	-	-	-	-	-	8	15	-	-
Tal3c	-	-	-	-	-	-	-	-	-	-	-	-	-	-	-	-
Tal1c	-	-	-	-	-	-	5	14	7	9	-	-	-	-	-	11
Xo1	-	-	4	6	3	6	-	-	-	-	-	-	-	-	-	-
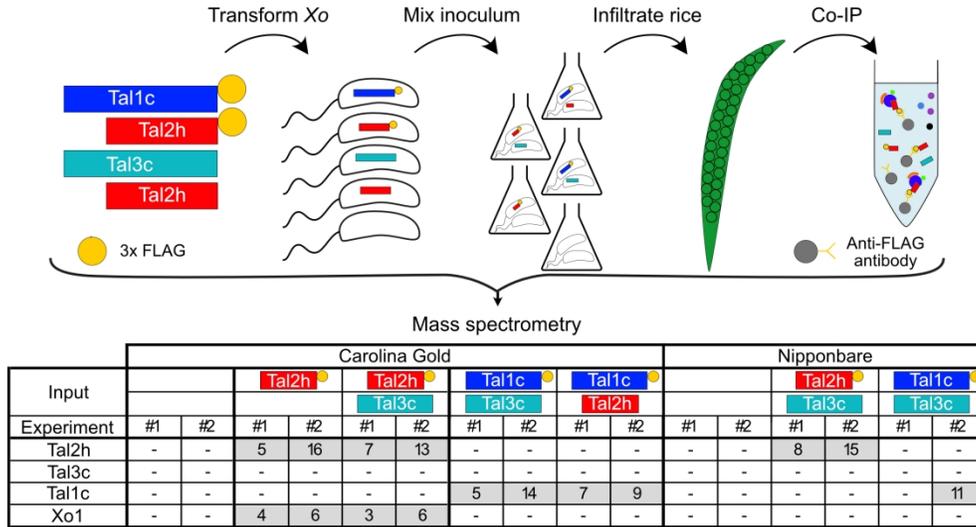
Fig. 4. Xo1 co-immunoprecipitates with Tal2h. Top, strategy used for co-immunoprecipitation (Co-IP) of truncTALE Tal2h or TALE Tal1c and any interactors. Plasmid borne expression constructs for Tal2h or Tal1c with a C-terminal 3x FLAG tag, as well as untagged Tal2h and a second TALE,Tal3c were introduced into Xanthomonas oryzae strain X11-5. Paired combinations of the transformants with each other or with the untransformed control strain, or the control strain alone, were co-infiltrated into leaves of rice varieties Carolina Gold and Nipponbare at a final OD600 0.5 for each transformant. Samples were collected 48 hours after inoculation, ground, and sonicated before Co-IP using anti-FLAG agarose beads. After elution and SDS-PAGE separation, proteins between approximately 60 and 300 kDa were eluted, digested and analyzed by mass spectrometry. The experiment was conducted twice. Bottom, co-IP results. For each immunoprecipitate, the numbers of unique peptides detected that matched Tal2h, Tal3c, Tal1c, or Xo1 in each experiment are shown. "-" indicates that ≤ 2 unique peptides were detected.

Cloning of the rice *Xo1* resistance gene and interaction of the Xo1 protein with the defense-suppressing *Xanthomonas* effector Tal2h

Andrew C. Read,[1][†] Mathilde Hutin,[1,2][†] Matthew J. Moscou,[3] Fabio C. Rinaldi,[1] and Adam J. Bogdanove[1]*

[1] Plant Pathology and Plant-Microbe Biology Section, School of Integrative Plant Science, Cornell University, Ithaca, NY 14853
[2] IRD, CIRAD, Université Montpellier, IPME, 34000 Montpellier, France
[3] The Sainsbury Laboratory, University of East Anglia, Norwich Research Park, Norwich, NR4 7UK, United Kingdom
[†] These authors contributed equally.
* Current address for F. C. Rinaldi: Vertex Pharmaceuticals, 50 Northern Avenue, Boston, MA 02210

Corresponding author: A. J. Bogdanove; ajb7@cornell.edu

Supplemental Text and Figures

Materials and methods

Fig. S1. Confirmation of CFBP7331(EV) and CFBP(p2h) inoculum on Nipponbare and Carolina Gold plants.

Fig. S2. Symptoms on Carolina Gold and Nipponbare leaves caused by inoculum used for the co-IP experiments.

Fig. S3. Western blot of immunoprecipitates using anti-TALE antibody.

Fig. S4. SDS-PAGE of immunoprecipitates and size range excised for mass spectrometry.

Supplemental references

Supplemental Materials and methods

Generation and testing of Xo1₁₁ transgenic Nipponbare

The binary transformation plasmid pAR902, containing the $Xo1_{11}$ promoter sequence, a Kozak sequence, the genomic $Xo1_{11}$ gene body, and a 35S terminator, was generated through several steps. Genomic $Xo1_{11}$ was amplified in two parts using oligo pairs 2492/2420 and 2421/2489. Amplicons were ligated into backbone vector pDONR221 following digestion with *Not*I, *Sph*I, and *Asc*I. This cloning strategy resulted in an undesired frameshift downstream of the coding sequence that made the clone incompatible with Gateway destination vectors. The frameshift was corrected by amplifying a small fragment with oligo pair 2644/2645 then ligating it into the *Cla*I/*Asc*I digested parent plasmid. A Kozak consensus sequence was introduced by QuickChange (Agilent) using primer pair 3267/3268. The 993 bp region upstream of the $Xo1_{11}$ start codon was amplified with oligo pair 3080/3082 and BP Gateway cloned into pDONR P4P1r (ThermoFisher). The plasmids containing the promoter sequence, the genomic $Xo1_{11}$ sequence, and a pDONR P2rP3 with a 35S terminator were LR Gateway cloned into the binary Gateway destination plasmid pKm43GW (Karimi et al., 2005).

Sequence confirmed pAR902 was electroporated into *Agrobacterium tumefaciens* strain EHA101 for transformation of japonica rice cultivar Nipponbare, which was performed by the Cornell University Plant Transformation Facility.

T0 regenerants were transferred to 4 inch pots containing LC-1 soil mixture (Sungro) and moved to a PGC15 (Percival Scientific) growth chamber ~60 cm below a combination of fluorescent and incandescent bulbs providing ~1000 µmoles/m^2/s measured at 15 cm, under a cycle of 12 h light at 28°C and 12 h dark at 25°C. Wildtype Nipponbare and Carolina Gold Select seeds were sown to serve as bacterial inoculation controls.

Xanthomonas oryzae pv. oryzicola strain CFBP7331 transformed with empty vector (pAC99; Cernadas et al., 2014) or p2h (Read et al., 2016) were grown overnight in liquid GYE with appropriate antibiotics at 28°C with shaking. Overnight cultures were pelleted, washed once, and resuspended in 10 mM $MgCl_2$ to an OD_{600} of 0.4 prior to infiltration using a needleless syringe (Reimers et al., 1992). Inoculated plants were maintained in the growth chamber under the above described conditions. Leaves were photographed on a light box.

Gene expression analysis

For *Xo1*, RNAseq data for mock-inoculated (SRR9320033, SRR9320038, SRR9320039), CFBP7331(EV)-inoculated (SRR9320035, SRR9320036, SRR9320037) and CFBP7331(p2h)-inoualted (SRR9320034, SRR9320040, SRR9320041) Carolina Gold Select plants (Read et al., 2020) were downloaded from the NCBI Sequence Read Archive. Reads were aligned to the MSU v7 Nipponbare reference genome annotation using the "—quantMode GeneCounts" option in STAR (Dobin et al., 2013). STAR output was used in DESEQ2 (Love et al., 2014) to determine differentially expressed genes (DEGs) in CFBP7331(EV) and CFBP7331(EV) compared to mock.

For *Pia*, NCBI GEO2R (Smyth, 2004; Davis and Meltzer, 2007) was used to identify DEGs from microarray data of rice line NP/Pia expressing the rice blast

resistance gene *Pia* (GEO GSE62893). Those data had been collected 24 hpi following mock-inoculation (GSM1535715, GSM1535731, GSM1535750) or inoculation with avirulent *Magnoporthe oryzae* strain P91-15B, race 001.0 (GSM1535711, GSM1535727, GSM1535743) (Tanabe et al., 2014).

For *Rxo1*, NCBI GEO2R (Smyth, 2004; Davis and Meltzer, 2007) was used to identify DEGs from microarray data of transgenic rice expressing the maize NLR gene *Rxo1* (GEO GSE19239) (Zhou et al., 2010). Data had been collected 48 hpi following mock-inoculation (GSM476772, GSM476773, GSM476774) or inoculation with avirulent Xoc strain FJR5 (GSM476769, GSM476770, GSM476771).

For *Xa23*, DEGs were as reported in a previous RNAseq analysis of rice variety CBB23 inoculated with strain PXO99A compared with mock inoculated CBB23 at 24 hpi (Tariq et al., 2018).

DEGs with log_2-fold change between -1 and 1 or with *p*-value >0.05 were excluded from the analysis. Heatmaps were generated in R version 3.6.3 using the package Superheat (Barter and Yu, 2018).

Principal component analysis was performed in R using the log fold-change values of differentially expressed defense genes between inoculated and mock-inoculated samples in the four data sets. In total, 181 genes were used in the analysis.

Localization of Xo1

The expression construct for green fluorescent protein fused to the N-terminus of Xo1 was generated by LR Gateway recombination between the $Xo1_{11}$ entry vector and pGWB6 (Nakagawa et al., 2007). Monomeric red fluorescent protein fusions to the N-termini of Tal1c and Tal2h were generated by LR Gateway cloning of *tal1c* and *tal2h* entry plasmids with pGWB455 (Tanaka et al., 2011). Empty pGWB455 was used as the free mRFP control construct. Expression constructs were electroporated into *A. tumefaciens* strain GV3101. Overnight cultures grown at 28°C in LB broth with antibiotic were pelleted and washed in infiltration buffer (10 mM MES, pH 5.6, 10 mM $MgCl_2$, and 150 μM acetosyringone). Washed pellets were resuspended in infiltration buffer, adjusted to OD_{600} 1.0, and mixed such that each strain was present at OD_{600} 0.4. Each mixture also contained GV3101 carrying an expression construct for the silencing suppressor p19 at OD_{600} 0.2. Mixtures were incubated for 4 hours at room temperature before blunt syringe infiltration of 4-week-old *Nicotiana benthamiana* leaves. Plants were left on the bench under fluorescent light for three days. Then, leaf discs were punched from the infiltrated area and observed with a Zeiss 710 confocal microscope at the Cornell Biotechnology Core Facility. GFP was imaged with excitation 488 nm and detection at 498-532 nm, while mRFP was imaged with excitation 561 nm and detection at 606 to 621 nm. Maximum intensity projections were generated in FIJI (Schindelin et al., 2012).

Co-immunoprecipitation, western blot analysis, and mass spectrometry

Plasmid pFR339 encoding Tal2h:3xFLAG was constructed by inserting a gBlock fragment at the restriction sites *Aat*II and *EcoR*V in-frame with *tal2h* in the plasmid pAR009_2h (Read et al., 2016) The gBlock encodes a fragment of the C-terminal domain of Tal2h followed by three tandem FLAG epitope tags. Plasmid pFR340 encoding Tal1c:3xFLAG was constructed by inserting a gBlock fragment at the

restriction sites *Bbv*CI and *Eco*RV in-frame with *tal1c* in the plasmid pAR009_1c (Read et al., 2016). The gBlock encodes a fragment of the C-terminal domain of Tal1C followed by three tandem FLAG epitope tags. gBlocks were synthesized by Integrated DNA Technologies. pFR339 and pFR340 were used as entry vectors to transfer the coding sequences into *Xanthomonas* expression vector pKEB31 (Cermak et al., 2011) by Gateway LR reaction (ThermoFisher Scientific). These constructs were transformed by electroporation into the TALE-deficient *X.oryzae* strain X11-5A (Triplett et al., 2011).

Nipponbare and Carolina Gold Select plants were grown in a growth chamber under cycles of 12 hours of light at 28°C and 75-80% relative humidity (RH), and 12 hours of dark at 25°C, and inoculated by syringe infiltration (Reimers et al., 1992) at 5 weeks old. For inoculation, individual bacterial suspensions containing each strain were made in 10 mM MgCl$_2$ at an OD$_{600}$ of 1, and mixed at equal volume to obtain the final suspensions for co-infiltration. A total of ten leaves with 60 to 80 tandem infiltration spots per leaf were inoculated for each co-inoculum. Leaves were collected 48 hpi and immediately frozen in liquid nitrogen.

Leaves frozen in liquid nitrogen were finely ground with a mortar and pestle. Three grams of leaf tissue were resuspended in 3 mL of GTEN extraction buffer (10% glycerol, 25 mM Tris pH 7.5, 1 mM EDTA, 150 mM NaCl) with 2% w/v polyvinylpolypyrrolidone, 1x protease inhibitor cocktail (Sigma Aldrich), and 0.1% Tween 20. Insoluble debris was pelleted by centrifugation at 3,000 x g for 20 min at 4°C. Samples were sonicated on ice and a second centrifugation at 20,000 x g for 20min at 4°C was done before transferring the supernatant to a new tube and adjusting to 2 mL with immunoprecipitation buffer (GTEN, with 0,1% Tween 20). EZview Red ANTI-FLAG M2 Affinity gel (Sigma Aldrich) was washed 2 times with 5 volumes of IP buffer and resuspended in the original volume. 5 µl of the suspension was added to each sample and the samples incubated with mixing by turning end-over-end for 2 h at 4°C. Resin was washed seven times in IP buffer, then bound proteins were eluted with 40 µl of 1x SDS Laemmli sample buffer without reducing agent. 1x dithiothreitol (DTT) was then added to each eluate and the samples incubated for 10 min at 95°C.

For western blotting, a 5 µl aliquot of each sample was resolved by 7.5% Tris-Glycine SDS-PAGE (Bio-Rad). Proteins were transferred to a membrane using the Trans-Blot Turbo Transfer System (Bio-Rad). Immunoblotting was performed using standard procedures. TALEs were detected with a 1:5000 diluted primary anti-TALE rabbit polyclonal antibody and a 1:1000 diluted secondary HRP conjugated goat anti-rabbit IgG antibody (Thermo Fisher). TALEs were visualized by chemiluminescence using the Clarity ECL substrate (Bio-Rad). The anti-TALE antibody was raised by Pocono Rabbit Farm and Laboratory (Canadensis, PA) using a 3 mg/ml sample of a dTALE expressed in *E. coli* and affinity-purified as described previously (Rinaldi et al., 2017). The antiserum was tested for specificity, and a dilution of 1:5000 was determined to be optimal for westernblot immunodetection of TALEs. Aliquots were preserved in -80°C in the presence of sodium azide.

Next, 30 µl of eluate from each immunoprecipitate were loaded in a 4-20% Tris Glycine SDS-PAGE stain free gel (Bio-Rad). The gel was stained using SYPRO Ruby protein gel stain (Invitrogen) following manufacturer instructions. The portion of each lane spanning molecular weight markers from 60 kDa to approximately 300 kDa was excised for mass spectrometry analysis. The excised gel fragments were subjected to

in-gel digestion followed by extraction of the tryptic peptide as reported previously (Yang et al., 2007). The gel pieces were washed consecutively with 600 µL distilled/deionized water followed by 50 mM ammonium bicarbonate, 50% acetonitrile (ACN), and finally 100% ACN. The dehydrated gel pieces were reduced with 250 µL of 10 mM DTT in 100 mM ammonium bicarbonate for 1 hour at 56 °C, then alkylated with 250 µL of 55 mM iodoacetamide in 100 mM ammonium bicarbonate at room temperature in the dark for 45 minutes.Wash steps were repeated as described above. The gel slices were then dried and rehydrated with trypsin (Promega) at an estimated 1:3 w/w ratio in 50 mM ammonium bicarbonate and 10% ACN and incubated at 37 °C for 18 h. The digested peptides were extracted twice with 200 µl of 50% ACN and 5% formic acid (FA) and once with 200 µl of 75% ACN and 5% FA. For each sample, extracts were combined and filtered with a Costar Spin-X 0.22 µm spin filter (Corning) and dried in a speed vacuum. Each sample was reconstituted in 2% ACN and 0.5% FA prior to LC MS/MS analysis.

Nano LC-ESI-MS/MS analysis was carried out using an Orbitrap Fusion Tribrid mass spectrometer (Thermo-Fisher Scientific) equipped with a nanospray Flex Ion Source and coupled with a Dionex UltiMate 3000 RSLCnano system (Thermo-Fisher Scientific) (Thomas et al., 2017; Yang et al., 2018). For each reconstituted sample, 8 µl were injected onto a PepMap C-18 RP nano trapping column (5 µm, 100 µm i.d x 20 mm) at 15 µL/min flow rate for rapid sample loading and then separated on a PepMap C-18 RP nano column (2 µm, 75 µm x 25 cm) at 35 °C. The tryptic peptides were eluted in a 60 min gradient of 5% to 38% ACN in 0.1% FA at 300 nL/min, followed by a 7 min ramping to 90% ACN-0.1% FA and an 8 min hold at 90% ACN-0.1% FA. The column was re-equilibrated with 0.1% FA for 25 min prior to the next run. The Orbitrap Fusion was operated in positive ion mode with spray voltage set at 1.6 kV and source temperature at 275°C. External calibration for FT, IT and quadrupole mass analyzers was performed. In data-dependent acquisition (DDA) analysis, the instrument was operated using FT mass analyzer in MS scan to select precursor ions followed by 3 sec "Top Speed" data-dependent CID ion trap MS/MS scans at 1.6 m/z quadrupole isolation for precursor peptides with multiple charged ions above a threshold ion count of 10,000 and normalized collision energy of 30%. MS survey scans at a resolving power of 120,000 (fwhm at m/z 200), for the mass range of m/z 375-1575. Dynamic exclusion parameters were set at 40 sec of exclusion duration with ±10 ppm exclusion mass width. All data were acquired under Xcalibur 3.0 operation software (Thermo-Fisher Scientific).

The raw DDA files for CID MS/MS were queried against peptide databases using Proteome Discoverer (PD) 2.2 software (Thermo Fisher Scientific) using the Sequest HT algorithm. The PD 2.2 processing workflow containing an additional node of Minora Feature Detector for precursor ion-based quantification was used for protein identification. The databases were generated from the *X. oryzae* strain X11-5A genome, encoding 3,546 proteins (Triplett et al., 2011), plus Tal1c, Tal2h, and Tal3c; the Nipponbare genome (MSU 7; Kawahara et al., 2013), containing 47,418 protein entries; and the Carolina Gold Select genome (Read et al., 2020). For the Carolina Gold Select genome, we reannotated by using hisat2 (Kim et al., 2019) to map to the genome the RNAseq reads we generated previously (Read et al., 2020), then cufflinks (Trapnell et al., 2012) to build gene models. This resulted in 33,956 protein entries. We added the

$Xo1_{11}$ gene model we predicted previously based on comparative structural analysis (Read et al., 2020). To generate the peptide database, two-missed trypsin cleavage sites were allowed. The peptide precursor tolerance was set to 10 ppm, and fragment ion tolerance was set to 0.6 Da. For the database search, variable modification of methionine oxidation, deamidation of asparagines/glutamine, and fixed modification of cysteine carbamidomethylation were set. Only high confidence peptides defined by Sequest HT with a 1% FDR by Percolator were considered for the peptide identification. The final protein IDs contained protein groups that were filtered with at least 2 peptides per protein. The precursor abundance intensity for each peptide identified by MS/MS in each sample was automatically determined and the unique peptides for each protein in each sample were summed and used for calculating the protein abundance by PD 2.2 software without normalization.

Plasmids used

Cloning *Xo1*

Plasmid	Description	Purpose	Reference
pKM43GW	Binary Gateway destination vector, Km[r]	destination	(Karimi et al., 2005)
pAR902	Binary Gateway destination vector pKM43GW containing the $Xo1_{11}$ promoter, $Xo1_{11}$ sequence of pDONR221:KozXo1, and 35S terminator, Sp[r]	transformation	This study
pDONR221:KozXo1	pDONR221 entry vector containing a 'CACC' Kozak sequence immediately upstream of the genomic sequence of $Xo1_{11}$ with stop codon deleted, Km[r]	intermediate	This study
Intermediate:Xo1_1	Genomic clone of $Xo1_{11}$ with stop codon deleted. Note that cloning strategy resulted in frame-shift for any C-terminal fusions and construct does not include Kozak sequence, Km[r]	intermediate	This study
Intermediate:Xo1_2	Same as Intermediate:Xo1_1, but C-terminal frame-shift was corrected, Km[r]	intermediate	This study
pDONR41:Xo1Promoter	pDONR_P4-P1r containing the 1kb genomic sequence upstream of $Xo1_{11}$, Km[r]	intermediate	This study
pDONR_P4-P1r	donor vector with attP4 and attP1 (reversed) sites, Km[r], Cm[r]	intermediate	Invitrogen
pDONR23:35St	pDONR_P2r-P3 containing an in-frame stop codon followed by a 35S terminator, Km[r]	intermediate	(Ivanov and Harrison, 2014)
pDONR_P2r-P3	donor vector with attP2 (reversed) and attP3 sites, Km[r], Cm[r]	intermediate	Invitrogen

Inoculation assay

Plasmid	Description	Purpose	Reference
pKEB31	pDD62 derivative containing Gateway destination vector cassette (Invitrogen) between *Xba*I and *Bam*HI sites, Tc^r	expression	(Cermak et al., 2011)
pAC99	pKEB31 containing *tal1c* of BLS256 missing the *Sph*I repeat-encoding fragment, Tc^r	expression	(Cernadas et al., 2014)
pKEB31-8-2h	pKEB31 containing Gateway fragment of pAR008-2h, Tc^r	expression	(Read et al., 2016)

Localization

Plasmid	Description	Purpose	Reference
pGWB455	Binary Gateway destination vector for transformation or transient expression of mRFP-tagged proteins, Sp^r, Cm^r	intermediate/ expression	(Nakagawa et al., 2007; Tanaka et al., 2011)
pGWB6	Binary Gateway destination vector for transformation or transient expression of GFP-tagged proteins, Km^r, Cm^r	intermediate/ expression	(Nakagawa et al., 2007)
pGWB455:Tal1c	Binary vector pGWB455 containing mRFP fusion at N-terminus of Tal1c from pAR009-1c, Sp^r	expression	This study
pAR008-2h	pAR008 containing the *Aat*II-*Sph*I CRR of tal2h, Ap^r	intermediate	(Read et al., 2016)
pAR009-1c	pAR009 containing the *Aat*II-*Sph*I CRR of tal1c, Ap^r	intermediate	(Read et al., 2016)
pGWB455:Tal2h	Binary vector pGWB455 containing mRFP fusion at N-terminus of Tal2h from pAR008-2h, Sp^r	expression	This study
pGWB6:Xo1	Binary vector pGWB6 containing GFP fusion at N-terminus of genomic $Xo1_{11}$ sequence from Intermediate:Xo1_2, Km^r	expression	This study

Co-IP

Plasmid	Description	Purpose	Reference
pTal1c-3xFLAG	Tal1c sequence from pAR009-1c with C-terminal 3xFLAG tag in pKEB31 expression backbone, Tc^r	expression	This study
pTal2h-3xFLAG	Tal2h sequence from pAR008-2h with C-terminal 3xFLAG tag in pKEB31 expression backbone, Tc^r	expression	This study

Oligonucleotides used

Oligo	Sequence	Purpose
b2492	CAAAAAAGCAGGCTCCGCGGCCGCCACCAA AATGGAGGATGTGGAAGCCGGTTTGC	Forward primer for amplifying *Xo1*$_{11}$ genomic sequence - contains NotI site
b2420	TCATTACCAAAAGCATGCACTTTAAATAGTGA	Reverse primer for amplifying *Xo1*$_{11}$ genomic sequence - contains SphI site
b2421	TGGTCACTATTTAAAGTGCATGCTTTTGGTAA	Forward primer for amplifying *Xo1*$_{11}$ genomic sequence - contains SphI site
b2489	AGAAAGCTGGGTCGGCGCGCCGACAATGCA TTGGAGCGGATT	Reverse primer for amplifying *Xo1*$_{11}$ genomic sequence - contains AscI site
b2644	CGACATCGATGACCCCTCTATCC	Forward primer to fix *Xo1*$_{11}$ C-terminus frame-shift - contains ClaI site
b2645	GTCGGCGCGCCCGTTCACATATCCCCCATT AATTTTG	Reverse primer to fix *Xo1*$_{11}$ C-terminus frame-shift - contains AscI site
b3267	CACCATGGAGGAGGTGGAAGCC	Forward primer to add 'CACC' Kozak sequence
b3268	GAAGCCTGCTTTTTTGTACAAAG	Reverse primer to add 'CACC' Kozak sequence
b3080	GGGGACAACTTTGTATAGAAAAGTTGCCTCG AGGGTATAGACCATATTTCCCCTG	Forward primer to amplify and clone *Xo1*$_{11}$ promoter sequence
b3082	GGGGACTGCTTTTTTGTACAAACTTGCGGAA CAGGAGCAGTCCTTGGACTG	Reverse primer to amplify and clone *Xo1*$_{11}$ promoter sequence
gBlock 2h	CTGCTTCGGCGGACGTCCTGCCCCGCATTC AAGGAAGAGGAAATCGCATGATGGATCCGG AGACTACAAAGACCATGACGGTGATTATAAA GATCATGACATCGATTACAAGGATGACGATG ACAAGTCCGGATGAAAGGGCGAATTCGACC CAGCTTTCTTGTACAAAGTTGGCATTATAAG AAAGCATTGCTTATCAATTTGTTGCAACGAA CAGGTCACTATCAGTCAAAATAAAATCATTAT TTGCCATCCAGCTGATATCCCCTATAGTGAG T	gBlock to insert FLAG tag at C-terminus of pAR008_2h

| gBlock 1c | CTGCATTTGCCCCTCAGCTGGAGGGTAAAA CGCCCGCGTACCAGGATCTGGGGCGGCCT CCCGGATCCTGGTACGCCCATGGCTGCCGA CCTGGCAGCGTCCAGCACCGTGATGTGGGA ACAAGATGCGGACCCCTTCGCAGGGGCAGC GGATGATTTCCCGGCATTCAACGAAGAGGA ACTCGCATGGTTGATGGAGCTATTGCCTCAG GGATCCGGAGACTACAAAGACCATGACGGT GATTATAAAGATCATGACATCGATTACAAGG ATGACGATGACAAGTCCGGATGAAAGGGCG AATTCGACCCAGCTTTCTTGTACAAAGTTGG CATTATAAGAAAGCATTGCTTATCAATTTGTT GCAACGAACAGGTCACTATCAGTCAAAATAA AATCATTATTTGCCATCCAGCTGATATCCCCT ATAGTGAGT | gBlock to insert FLAG tag at C-terminus of pAR009_1c |

Xo1 RNAseq analysis

```
#SRR files downloaded from ENA -- repeated for all SRR files
wget ftp://ftp.sra.ebi.ac.uk/vol1/fastq/SRR932/004/SRR9320034/SRR9320034_1.fastq.gz

#Renaming files
mv SRR9320033.fastq.gz Mock3.fastq.gz
mv SRR9320034.fastq.gz 2h1.fastq.gz
mv SRR9320035.fastq.gz EV3.fastq.gz
mv SRR9320036.fastq.gz EV2.fastq.gz
mv SRR9320037.fastq.gz EV1.fastq.gz
mv SRR9320038.fastq.gz Mock2.fastq.gz
mv SRR9320039.fastq.gz Mock1.fastq.gz
mv SRR9320040.fastq.gz 2h3.fastq.gz
mv SRR9320041.fastq.gz 2h2.fastq.gz

#Nipponbare reference genome and annotation downloaded from MSU version 7.0
#genome = all.chrs.fasta
#annotation = all.gff3

#Annotation converted to .gtf and renamed
gffread all.gff3 -T -o Nippo.gtf

#The genome was indexed for STAR
STAR --runMode genomeGenerate --runThreadN 7 --genomeDir Nippo_Index --genomeFastaFiles
allchrs.fasta --sjdbGTFfile Nippo.gtf --sjdbOverhang 100

#Each pair of reads was aligned to the Nipponbare reference -- repeated for all
STAR --runThreadN 8 --runMode alignReads --genomeDir Nippo_Index/ --readFilesIn EV3_1.fastq.gz
EV3_2.fastq.gz --outSAMtype BAM SortedByCoordinate --outFileNamePrefix EV3 --readFilesCommand
zcat

#Concatenate the count columns from all STAR output to get ready for DESEQ2
paste 2h1ReadsPerGene.out.tab 2h2ReadsPerGene.out.tab 2h3ReadsPerGene.out.tab
EV1ReadsPerGene.out.tab EV2ReadsPerGene.out.tab EV3ReadsPerGene.out.tab
```

```
Mock1ReadsPerGene.out.tab Mock2ReadsPerGene.out.tab Mock3ReadsPerGene.out.tab | cut -
f1,2,6,10,14,18,22,26,30,34 | tail -n +5 > gene_count.txt

#Create a sample file to link treatment to count - it should look like this:
#Sample    Trtmnt
#2h1    2h
#2h2    2h
#2h3    2h
#EV1    EV
#EV2    EV
#EV3    EV
#Mock1    Mock
#Mock2    Mock
#Mock3    Mock

#With these files I was able to run DESEQ2 in Rstudio V1.2.5033
#note that this includes analysis such as the PCA that are not displayed in the manuscript

matrixFile <- "gene_count.txt"
sampleFile <- "samples.txt"
cts <- as.matrix(read.csv(matrixFile, sep="\t", row.names=1, header=FALSE))
coldata <- read.csv(sampleFile, sep="\t", row.names=1, header=TRUE)
#head(coldata)
#head(cts)
colnames(cts) <- rownames(coldata)

if (!requireNamespace("BiocManager", quietly = TRUE))
  install.packages("BiocManager")
if (!requireNamespace("DESeq2", quietly = TRUE))
  BiocManager::install("DESeq2")
if (!requireNamespace("dplyr", quietly = TRUE))
  install.packages("dplyr")
if (!requireNamespace("pheatmap", quietly = TRUE))
  install.packages("pheatmap")
if (!requireNamespace("tidyverse", quietly = TRUE))
  install.packages("tidyverse")

library(DESeq2)
library(dplyr)
library(pheatmap)
library(tidyverse)

dds <- DESeqDataSetFromMatrix(countData=cts, colData=coldata, design =~ Trtmnt)
dds.data <- DESeq(dds)
head(dds.data)

vsd <- vst(dds, blind=FALSE)
pca =  plotPCA(vsd, intgroup = "Trtmnt")
pca
pca$data

#Mock_vs_2h - this is Mock vs Disease
Mock.2h <- results(dds.data, contrast=c("Trtmnt", "Mock", "2h"), alpha = 0.05)
Mock.2h %>% head()
write.csv(Mock.2h, file = paste0( "Mockvs2h_results.csv"))
```

```
#Mock_vs_EV - this is Mock vs HR
Mock.EV <- results(dds.data, contrast=c("Trtmnt", "Mock", "EV"), alpha = 0.05)
Mock.EV %>% head()
write.csv(Mock.EV, file = paste0( "MockvsEV_results.csv"))

#EV_vs_2h - This is HR vs Disease
EV.2h <- results(dds.data, contrast=c("Trtmnt", "EV", "2h"), alpha = 0.05)
EV.2h %>% head()
write.csv(EV.2h, file = paste0( "EVvs2h_results.csv"))

comp = as.data.frame(Mock.2h)

hmap.query = comp %>%
  rownames_to_column("genes") %>%
  filter(., padj < 0.05 & baseMean > 1000)

vsd.table = as.data.frame(assay(vsd))
hisat2-build reconciled_assembly_v4.fa reconciled_assembly_v4
```

Carolina Gold genome annotation

```
hisat2-build reconciled_assembly_v4.fa reconciled_assembly_v4
hisat2 --max-intronlen 20000 -k 1 -p 8 --no-softclip --dta-cufflinks -x reconciled_assembly_v4 -1
Mock_1_RNAseq_forward_paired.fq.gz -2 Mock_1_RNAseq_reverse_paired.fq.gz -S
Mock_1_RNAseq.cufflinks.sam > hisat2.Mock_1.cufflinks.log 2>&1 &
hisat2 --max-intronlen 20000 -k 1 -p 8 --no-softclip --dta-cufflinks -x reconciled_assembly_v4 -1
Mock_2_RNAseq_forward_paired.fq.gz -2 Mock_2_RNAseq_reverse_paired.fq.gz -S
Mock_2_RNAseq.cufflinks.sam > hisat2.Mock_2.cufflinks.log 2>&1 &
hisat2 --max-intronlen 20000 -k 1 -p 8 --no-softclip --dta-cufflinks -x reconciled_assembly_v4 -1
Mock_3_RNAseq_forward_paired.fq.gz -2 Mock_3_RNAseq_reverse_paired.fq.gz -S
Mock_3_RNAseq.cufflinks.sam > hisat2.Mock_3.cufflinks.log 2>&1 &

samtools view -F 4 -Shub Mock_1_RNAseq.cufflinks.sam > Mock_1_RNAseq.cufflinks.bam
samtools sort -o Mock_1_RNAseq.cufflinks.sorted.bam Mock_1_RNAseq.cufflinks.bam

samtools view -F 4 -Shub Mock_2_RNAseq.cufflinks.sam > Mock_2_RNAseq.cufflinks.bam
samtools sort -o Mock_2_RNAseq.cufflinks.sorted.bam Mock_2_RNAseq.cufflinks.bam

samtools view -F 4 -Shub Mock_3_RNAseq.cufflinks.sam > Mock_3_RNAseq.cufflinks.bam
samtools sort -o Mock_3_RNAseq.cufflinks.sorted.bam Mock_3_RNAseq.cufflinks.bam

samtools merge Mock_RNAseq.cufflinks.sorted.bam Mock_1_RNAseq.cufflinks.sorted.bam
Mock_2_RNAseq.cufflinks.sorted.bam Mock_3_RNAseq.cufflinks.sorted.bam

cufflinks -p 8 Mock_RNAseq.cufflinks.sorted.bam > cufflinks.log 2>&1 &
gffread transcripts_Mock.gtf -g reconciled_assembly_v4.fa -w transcripts_Mock.fa
TransDecoder.LongOrfs -t transcripts_Mock.fa
./interproscan.sh --output-dir . --input longest_orfs.pep --iprlookup --seqtype p --appl
Coils,Gene3D,ProSitePatterns,Pfam,PANTHER,SUPERFAMILY > longest_orfs_interproscan.log 2>&1 &

#this was repeated for the 2h and EV datasets
```

Heatmap and PCA generation in R

```
#Heatmap All HR DEGs
HR_NA=read.table("Table_S1_All_HR_DEGs.txt", sep="\t", header=TRUE, row.names=1)
HR_NA_matrix=data.matrix(HR_NA)
superheat(HR_NA_matrix, heat.na.col = "black", title="All HR DEGs",
      title.size = 8, grid.vline.col = "white")

#Heatmap Only GO:0006952
Def_DEGs=read.table("Table_S2_Defense_HR_DEGs.txt", sep="\t", header=TRUE, row.names=1)
Def_DEGs_matrix=data.matrix(Def_DEGs)
superheat(Def_DEGs_matrix, heat.na.col = "black", title="Defense DEGs",
      title.size = 8, grid.vline.col = "white")

#Heatmap to compare overlapping Defense GO HR and Disease
Overlap_GODEGs=read.table("Table_S3_CGS_Disease_and_HR_DEG_Overlap.txt", sep="\t",
header=TRUE, row.names=1)
Overlap_GODEGs_matrix=data.matrix(Overlap_GODEGs)
superheat(Overlap_GODEGs_matrix, heat.na.col = "black", title="Disease DEGs CGS Overlap",
      title.size = 8, grid.vline.col = "white")

#Principal Component Analysis
data = read.table(file="rice_pathogen_RNAseq.txt", sep="\t", header=T)
pcs=prcomp(t(x),center=T,scale.=T,retx=T)

postscript(file="rice_pathogen_RNAseq_v2.ps", width=4, height=6)
plot(pcs$x[,2],pcs$x[,1], xlab="", ylab="", main="")
dev.off()
```

Supplemental Figures
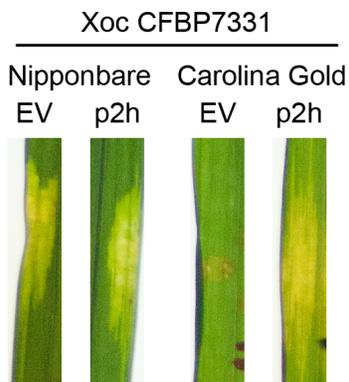
Fig. S1. Confirmation of CFBP7331(EV) and CFBP7331(p2h) inoculum on Nipponbare and Carolina Gold plants**.** Leaves were syringe-infiltrated with African Xoc strain CFBP7331 carrying either empty vector (EV) or *tal2h* (p2h) adjusted to OD_{600} 0.4, and incubated for 10 days to allow lesion expansion. Leaves were photographed on a light box. Resistance is apparent as HR (necrosis) at the site of inoculation and disease as expanded, translucent watersoaking.
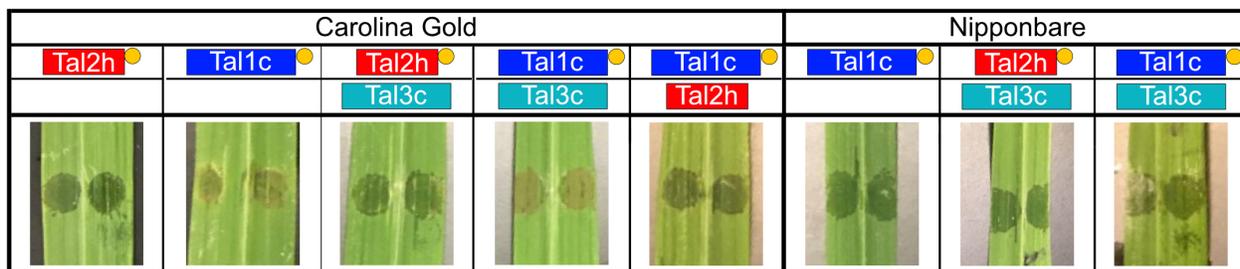
Fig. S2. Symptoms on Carolina Gold Select and Nipponbare leaves caused by inoculum used for the co-IP experiments. Photos were taken with overhead lighting 4 days after syringe infiltration. Resistance is apparent as HR (brown) and disease as watersoaking (dark green).
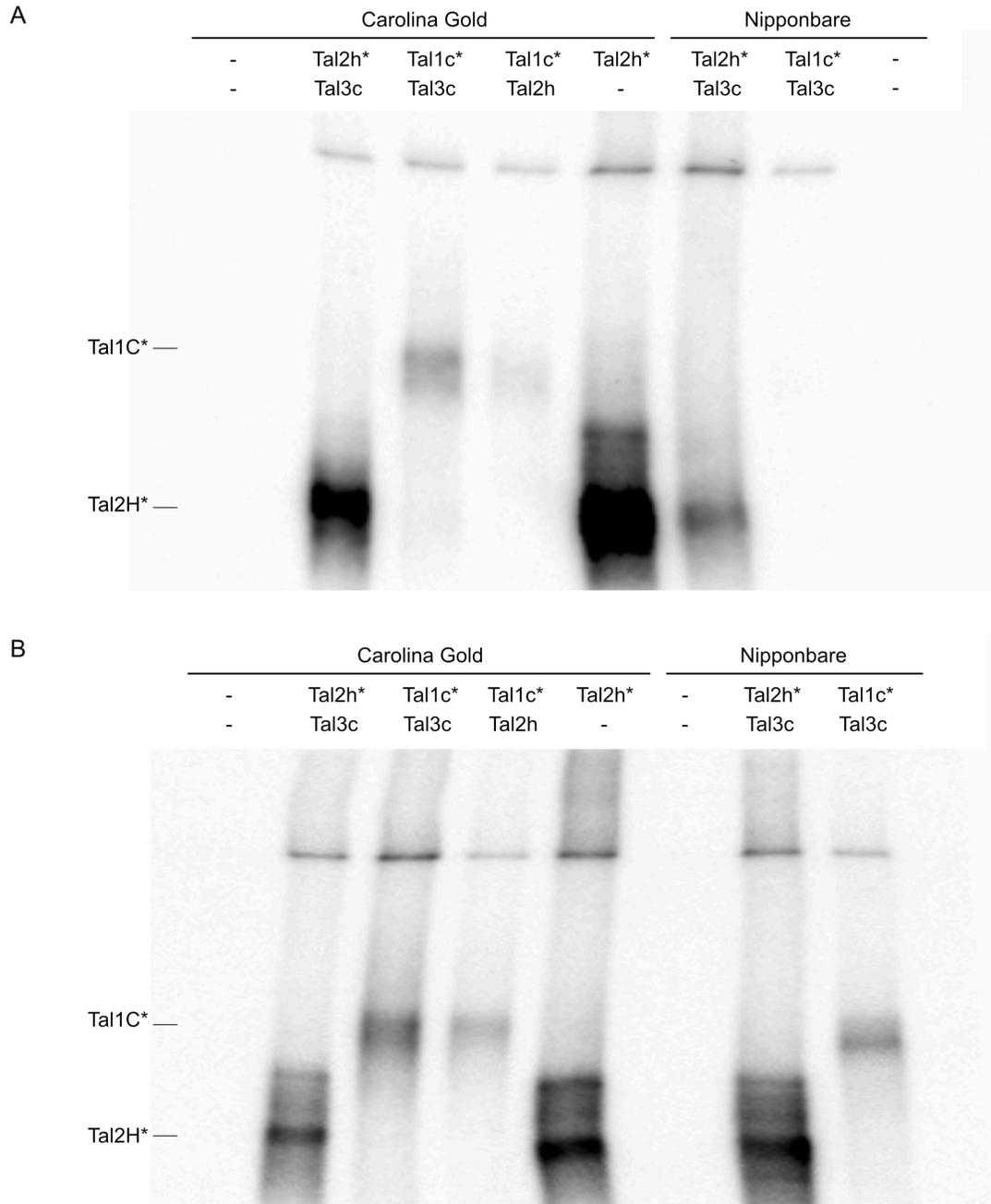
Fig. S3. Western blot of immunoprecipitates using anti-TALE antibody. Aliquots of the eluted immunoprecipitates from co-immunoprecipitation experiments 1 (A) and 2 (B) were resolved by 7.5% Tris-Glycine SDS-PAGE and probed with anti-TALE antibody. An asterisk indicates a 3x FLAG fusion.
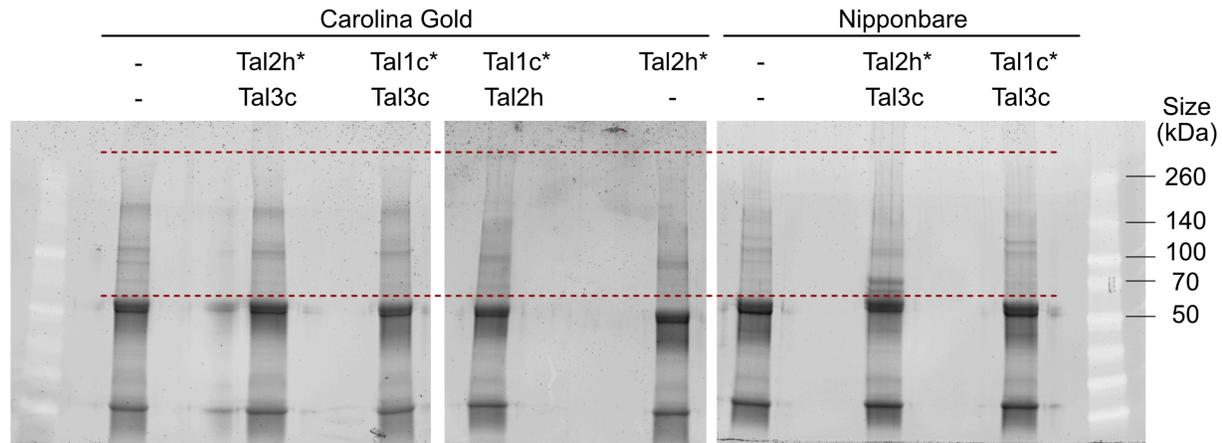
Fig. S4. SDS-PAGE of immunoprecipitates and size range excised for mass spectrometry.
A 4-20% polyacrylamide gel was used and proteins were stained using SYPRO Ruby. Samples were placed a lane apart to avoid cross-contamination. Red lines represent the region of the gel that were excised, containing proteins between approximately 60 and 300 kDa, and digested before mass spectrometry analysis. This gel is from the second co-immunoprecipitation experiment.

Supplemental References

Barter, R.L., and Yu, B. 2018. Superheat: An R package for creating beautiful and extendable heatmaps for visualizing complex data. J. Comput. Graph Stat. 27:910-922.

Cermak, T., Doyle, E.L., Christian, M., Wang, L., Zhang, Y., Schmidt, C., Baller, J.A., Somia, N.V., Bogdanove, A.J., and Voytas, D.F. 2011. Efficient design and assembly of custom TALEN and other TAL effector-based constructs for DNA targeting. Nucleic Acids Res. 39:e82.

Cernadas, R.A., Doyle, E.L., Nino-Liu, D.O., Wilkins, K.E., Bancroft, T., Wang, L., Schmidt, C.L., Caldo, R., Yang, B., White, F.F., Nettleton, D., Wise, R.P., and Bogdanove, A.J. 2014. Code-assisted discovery of TAL effector targets in bacterial leaf streak of rice reveals contrast with bacterial blight and a novel susceptibility gene. PLoS Path. 10:e1003972.

Davis, S., and Meltzer, P.S. 2007. GEOquery: a bridge between the Gene Expression Omnibus (GEO) and BioConductor. Bioinformatics 23:1846-1847.

Dobin, A., Davis, C.A., Schlesinger, F., Drenkow, J., Zaleski, C., Jha, S., Batut, P., Chaisson, M., and Gingeras, T.R. 2013. STAR: ultrafast universal RNA-seq aligner. Bioinformatics 29:15-21.

Ivanov, S., and Harrison, M.J. 2014. A set of fluorescent protein-based markers expressed from constitutive and arbuscular mycorrhiza-inducible promoters to

label organelles, membranes and cytoskeletal elements in *Medicago truncatula*. Plant J. 80:1151-1163.

Karimi, M., De Meyer, B., and Hilson, P. 2005. Modular cloning in plant cells. Trends Plant Sci. 10:103-105.

Kawahara, Y., de la Bastide, M., Hamilton, J.P., Kanamori, H., McCombie, W.R., Ouyang, S., Schwartz, D.C., Tanaka, T., Wu, J., and Zhou, S. 2013. Improvement of the *Oryza sativa* Nipponbare reference genome using next generation sequence and optical map data. Rice 6:4.

Kim, D., Paggi, J.M., Park, C., Bennett, C., and Salzberg, S.L. 2019. Graph-based genome alignment and genotyping with HISAT2 and HISAT-genotype. Nat. Biotechnol. 37:907-915.

Love, M.I., Huber, W., and Anders, S. 2014. Moderated estimation of fold change and dispersion for RNA-seq data with DESeq2. Genome Biol. 15:550.

Nakagawa, T., Suzuki, T., Murata, S., Nakamura, S., Hino, T., Maeo, K., Tabata, R., Kawai, T., Tanaka, K., Niwa, Y., Watanabe, Y., Nakamura, K., Kimura, T., and Ishiguro, S. 2007. Improved Gateway binary vectors: high-performance vectors for creation of fusion constructs in transgenic analysis of plants. Biosci. Biotechnol. Biochem. 71:2095-2100.

Read, A.C., Rinaldi, F.C., Hutin, M., He, Y.-Q., Triplett, L.R., and Bogdanove, A.J. 2016. Suppression of *Xo1*-mediated disease resistance in rice by a truncated, non-DNA-binding TAL effector of *Xanthomonas oryzae*. Front. Plant Sci. 7:1516.

Read, A.C., Moscou, M.J., Zimin, A.V., Pertea, G., Meyer, R.S., Purugganan, M.D., Leach, J.E., Triplett, L.R., Salzberg, S.L., and Bogdanove, A.J. 2020. Genome assembly and characterization of a complex zfBED-NLR gene-containing disease resistance locus in Carolina Gold Select rice with Nanopore sequencing. PLoS Genet. 16:e1008571.

Reimers, P.J., Guo, A., and Leach, J.E. 1992. Increased activity of a cationic peroxidase associated with an incompatible interaction between *Xanthomonas oryzae* pv. oryzae and rice *Oryza sativa*. Plant Physiol. 99:1044-1050.

Rinaldi, F.C., Doyle, L.A., Stoddard, B.L., and Bogdanove, A.J. 2017. The effect of increasing numbers of repeats on TAL effector DNA binding specificity. Nucleic Acids Res. 45:6960-6970.

Schindelin, J., Arganda-Carreras, I., Frise, E., Kaynig, V., Longair, M., Pietzsch, T., Preibisch, S., Rueden, C., Saalfeld, S., Schmid, B., Tinevez, J.Y., White, D.J., Hartenstein, V., Eliceiri, K., Tomancak, P., and Cardona, A. 2012. Fiji: an open-source platform for biological-image analysis. Nat. Methods 9:676-682.

Smyth, G.K. 2004. Linear models and empirical bayes methods for assessing differential expression in microarray experiments. Stat. Appl. Genet. Mol. Biol. 3:Article3.

Tanabe, S., Yokotani, N., Nagata, T., Fujisawa, Y., Jiang, C., Abe, K., Ichikawa, H., Mitsuda, N., Ohme-Takagi, M., Nishizawa, Y., and Minami, E. 2014. Spatial regulation of defense-related genes revealed by expression analysis using dissected tissues of rice leaves inoculated with *Magnaporthe oryzae*. J. Plant Physiol. Pathol. 2:1000135.

Tanaka, Y., Nakamura, S., Kawamukai, M., Koizumi, N., and Nakagawa, T. 2011. Development of a series of gateway binary vectors possessing a tunicamycin

resistance gene as a marker for the transformation of *Arabidopsis thaliana*. Biosci. Biotechnol. Biochem. 75:804-807.

Tariq, R., Wang, C., Qin, T., Xu, F., Tang, Y., Gao, Y., Ji, Z., and Zhao, K. 2018. Comparative transcriptome profiling of rice near-isogenic line carrying *Xa23* under infection of *Xanthomonas oryzae* pv. oryzae. Int. J. Mol. Sci. 19:717.

Thomas, C.J., Cleland, T.P., Zhang, S., Gundberg, C.M., and Vashishth, D. 2017. Identification and characterization of glycation adducts on osteocalcin. Anal. Biochem. 525:46-53.

Trapnell, C., Roberts, A., Goff, L., Pertea, G., Kim, D., Kelley, D.R., Pimentel, H., Salzberg, S.L., Rinn, J.L., and Pachter, L. 2012. Differential gene and transcript expression analysis of RNA-seq experiments with TopHat and Cufflinks. Nat. Protoc. 7:562-578.

Triplett, L.R., Hamilton, J.P., Buell, C.R., Tisserat, N.A., Verdier, V., Zink, F., and Leach, J.E. 2011. Genomic analysis of *Xanthomonas oryzae* isolates from rice grown in the United States reveals substantial divergence from known *X. oryzae* pathovars. Appl. Environ. Microbiol. 77:3930-3937.

Yang, Y., Anderson, E., and Zhang, S. 2018. Evaluation of six sample preparation procedures for qualitative and quantitative proteomics analysis of milk fat globule membrane. Electrophoresis 39:2332-2339.

Yang, Y., Thannhauser, T.W., Li, L., and Zhang, S. 2007. Development of an integrated approach for evaluation of 2-D gel image analysis: impact of multiple proteins in single spots on comparative proteomics in conventional 2-D gel/MALDI workflow. Electrophoresis 28:2080-2094.

Zhou, Y.L., Xu, M.R., Zhao, M.F., Xie, X.W., Zhu, L.H., Fu, B.Y., and Li, Z.K. 2010. Genome-wide gene responses in a transgenic rice line carrying the maize resistance gene *Rxo1* to the rice bacterial streak pathogen, *Xanthomonas oryzae* pv. oryzicola. BMC Genomics 11:78.